

A Wavelet-CNN Feature Fusion Approach for Detecting COVID-19 from Chest Radiographs

Md. Latifur Rahman¹, Nusrat Binta Nizam², Prasun Datta¹, Md. Moynul Hasan³, Taufiq Hasan², and Mohammed Imamul Hassan Bhuiyan¹

¹Dept. EEE, ²Dept. BME, ³Dept. NAME

^{1,2,3}Bangladesh University of Engineering and Technology, Dhaka-1205, Bangladesh

Email: alif.eee.buet@gmail.com, nusratbintanizam@ug.bme.buet.ac.bd, Prasundatta19961225@gmail.com, mmoynulhasan@ug.name.buet.ac.bd, taufiq@bme.buet.ac.bd and imamul@eee.buet.ac.bd

Abstract—Despite the combined effort, the COVID-19 pandemic continues with a devastating effect on the healthcare system and the well-being of the world population. With a lack of RT-PCR testing facilities, one of the screening approaches has been the use of chest radiography. In this paper, we propose an automatic chest x-ray image classification model that utilizes the pre-trained CNN architecture (DenseNet121, MobileNetV2) as a feature extractor, and wavelet transformation of the pre-processed images using the CLAHE algorithm and SOBEL edge detection. Our model can detect COVID-19 from x-ray images with high accuracy, sensitivity, specificity, and precision. The result analysis of different architectures and a comparison study of pre-processing techniques (Histogram Equalization and Edge Detection) are thoroughly examined. In this experiment, the Support Vector Machine (SVM) classifier fitted most accurately (accuracy 97.73%, sensitivity 97.84%, F1-score 97.73%, specificity 97.73%, and precision 98.79%) with a wavelet and MobileNetV2 feature sets to identify COVID-19. The memory consumption is also examined to make the model more feasible for telemedicine and mobile healthcare application.

Index Terms—COVID-19, Feature extraction, Wavelet transform, Histogram Equalization, Edge detection, DenseNet121, MobileNetV2

I. INTRODUCTION

The COVID-19 pandemic has been causing devastating effects in the health systems worldwide. It was declared a pandemic by the World Health Organization (WHO) in early March 2020 [1]. It is caused by the SARS-CoV-2 virus, which is a member of the Coronavirus family. It shares about 79% and 50% genomic similarity with SARS-CoV and MERS-CoV, respectively. COVID-19 is a highly contagious respiratory virus. The main symptoms of infected patients are fever, cough, fatigue, and gastrointestinal infection. The elderly and people with underlying diseases are more susceptible to the Coronavirus and can suffer from acute respiratory distress syndrome (ARDS) and cytokine storm at the end.

There are several testing protocols for the diagnosis of COVID-19 by WHO [2]. The standard method is RT-PCR. It is typically done by a nasopharyngeal swab, and the results can be obtained within a few hours to two days. Automated

assay from Abbott Diagnostics uses an isothermal nucleic acid amplification method [3]. Serology methods are in the stage of development [4]. RT-PCR is a time consuming, costly, laborious, and complicated process of testing. It has a positivity rate of 63% [5]. Many countries are suffering from incorrect detection of patients with COVID-19. Many patients are not being tested, and also the testing method needs much time. The high expense of the testing kit, insufficient amounts of testing kits, and professionals for sample collection and testing biosafety labs cause a delay in testing. This delay can increase the number of infected patients and can cause severe harm to infected patients.

The majority of COVID-19 radiographic images have similar features. Mainly the bilateral, multifocal, ground-glass opacities with peripheral or posterior distribution, in lower lobes, in the early stage, and pulmonary consolidation in the late stage are noticed in these images [6]–[10]. A chest x-ray is considered as one of the imaging methods for respiratory disease diagnosis. In the early stage of COVID-19 infection, the radiographic report may show normal, but in the late stages of infection, it may show several resemblances with pneumonia or acute respiratory distress syndrome. The main findings of chest x-ray radiographic images are bilateral multifocal consolidations progressing to the entire lungs and also pleural effusions. Though chest x-ray is a less sensitive modality (69%) [11] than CT images, its availability and cost-effectiveness can help in the diagnosis of COVID-19 both in developing and underdeveloped areas. It also can be an effective tool for teleradiology and portable radiography, which can further be used in telemedicine platforms for the improvement of treatment in remote areas. This rapid growth of medical image data quantity requires extensive and tedious efforts by the radiologists. An alternative solution is using machine learning (ML) techniques can thus be effective in assisting the radiologists in making the diagnostic decisions.

There are several machine learning methods available to identify COVID-19 from x-ray images. Automated COVID-19 detection from x-ray images using transfer learning method

has achieved accuracy 96.78% on 2 class and 94.72% on 3 class using MobileNetV2 [12]. DarkCovidNet model has claimed accuracy of 98.08% and 87.02% for binary and multi-classes and has generated heatmaps that can help them to locate the affected regions on chest x-rays [13]. Another deep learning convolutional neural network (CNN) architecture, CovidNet has obtained 93.3% accuracy on the test dataset for 3 class classification [14]. A capsule network-based framework, COVID-CAPS, has achieved an accuracy of 95.7%, Sensitivity of 90%, Specificity of 95.8% [15]. CovXNet is a multi-dilation CNN which detects COVID-19 and pneumonia using transferable multi-receptive feature optimization and has claimed 90.2% accuracy for multiclass COVID/Normal/Viral/Bacterial pneumonia [16]. COVID-MobileXpert is another lightweight deep neural network which is designed on a framework including a pre-trained attending physician network for feature extraction and can perform on-device COVID-19 screening [17].

In this paper, we propose a two-stream approach for the classification of chest x-ray images of normal, pneumonia, and COVID-19 pneumonia. We utilize histogram normalization and edge detection as pre-processing steps. Subsequently, features are extracted in parallel using discrete wavelet transform and the DenseNet121/MobileNetV2 architecture, respectively. The combined features are then classified employing a support vector machine (SVM). The performance in classification is studied on publicly available data of 2,940 chest x-ray images containing 1000 normal, 1000 pneumonia, and 940 COVID-19 pneumonia cases using well-known metrics. It is shown that excellent performance can be achieved using both architectures with pre-processing and wavelet transform, MobileNetV2 yielding better results.

II. MATERIALS AND METHODS

A. Dataset

The data used in our experiments are collected from different open-access resources [18]–[20]. A total of 2,940 chest radiography images are accumulated, where 940 images are of COVID-19 case, 1000 of Pneumonia, and 1000 of Normal. 70% of data are used for training and 30% of data are used for validating the results. As the COVID-19 chest x-ray images are collected from different publicly available datasets, automatic analysis to find similar images and exclude duplicate images is done in this case.

B. Proposed Method

The model proposed method is depicted in Fig. 1.

1) *Pre-processing*: Pre-processing steps such as image enhancement and edge detection have been shown to improve performance in medical image analysis [21]. In this paper, the x-ray images are first converted to a suitable grayscale format and re-sampled to a size of 224×224 [22]. Next, the data is pre-processed using the CLAHE histogram equalization algorithm and edge detection using the SOBEL method. In this work, we use the Contrast Limited Adaptive Histogram Equalization (CLAHE), which reduces image variability by

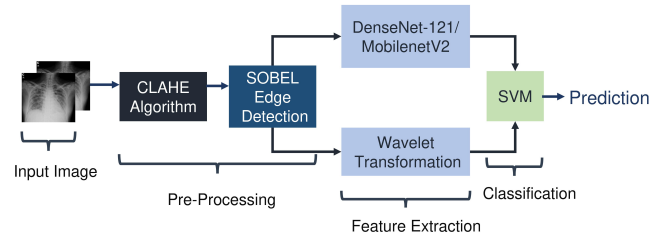


Fig. 1: A schematic flow-diagram of the proposed chest x-ray image classification method for COVID-19 detection.

clipping the image histogram at a predefined value before calculating the cumulative distribution function (CDF) and redistribute this part of the image equally among all the histogram bins [23], [24]. Next, we use the Sobel method for edge detection. The Sobel method is used to find sharp edges using thresholding the gradient [25].

2) *Wavelet Transformation*: An x-ray image is decomposed into horizontal, vertical, and diagonal sub-bands using the Haar wavelet. The extracted wavelet of the x-ray images coefficients are considered as input features to the SVM classifier since the single-level decomposition can yield image details in different directions which can enhance the classification. The coefficients in different sub-bands are then concatenated and converted to a 2D array.

3) *DenseNet121 Feature Extraction*: To improve the results, feature extraction is performed on edge detected image using a pre-trained DenseNet121 architecture. This network [26], is trained on the ImageNet dataset, renowned for pre-training most of the pre-trained model. DenseNet121 structure has 4 dense blocks on 224×224 input images. The initial convolution layer comprises 2k convolutions of size 7×7 with stride 2, where k is a hyperparameter denoting the growth rate of the network. The number of feature-maps in all other layers also follows from setting k. The input layer of this model takes an image in the size of $(224 \times 224 \times 3)$, and the output layer is a softmax prediction on 1000 classes. From the input layer, 16 blocks and the last ReLU layer is regarded as the feature extraction part of the model.

4) *MobileNetV2 Feature Extraction*: Similar to DenseNet121, feature extraction is again performed using a pre-trained MobileNetV2 architecture for better and simpler computation. This network [27], is trained on the ImageNet dataset, renowned for pre-training and deployment in different low-power, limited-computing devices [28]. The architecture of MobileNetV2 contains the initial fully convolution layer with 32 filters, followed by 19 residual bottleneck layer. As both DenseNet121 and MobileNetV2 are trained on the ImageNet dataset, input and output layers are the same. From the input layer, 16 blocks and the last ReLU layer is regarded as the feature extraction part of the model.

5) *Classifier*: In this experiment, the pre-trained models are used for extracting the features to create data frames. The data frames are divided into training (70%) and testing (30%)

TABLE I: Result analysis of 3 class classification for different setup with SVM classifier

Classifier	Accuracy	Sensitivity	Specificity	Precision	F1-Score
Wavelet	0.9206	0.9220	0.9206	0.9605	0.9209
Pre-processing + Wavelet	0.9274	0.9315	0.9274	0.9620	0.9270
DenseNet121	0.9671	0.9675	0.9671	0.9835	0.9671
Pre-processing + DenseNet121	0.9422	0.9421	0.9422	0.9709	0.9419
Pre-processing + DenseNet121 + Wavelet	0.9615	0.9627	0.9615	0.9807	0.9614
MobileNetV2	0.9501	0.9504	0.9501	0.9747	0.9500
Pre-processing + MobileNetV2	0.9569	0.9573	0.9569	0.9777	0.9567
Pre-processing + MobileNetV2 + Wavelet	0.9773	0.9784	0.9773	0.9879	0.9773

subset. The results shown in this paper are from the validation of these test data subset using support vector machine (SVM) classifier. The sigmoid kernel is used in this experiment to do the three-class classification using different feature sets.

III. RESULTS

Experiments are conducted using different feature sets and with/without pre-processing of image. The results of the validation using SVM classifier are provided in Table. I.

The proposed framework is implemented in TensorFlow and Keras. The system is accelerated by a Google Collaboratory cloud GPU Nvidia K80. The Adam optimizer is used while training, and the learning rate is set to $1e-4$. Using DenseNet121 and MobileNetV2 architecture, class activation heatmaps are generated. The highlighted sections in the images of pneumonia and COVID-19 x-ray in Fig. 2 indicates that these sections can be used as important features to detect pneumonia and COVID-19. These findings also matches the clinical notes of radiology image analysis [29], [30]. In Table I, using only wavelet features with pre-processing shows better accuracy than without pre-processing of images. Pre-processing improves the obtained features and thus improves the classification results. The results of DenseNet121 feature set are shown, where we can notice that pre-processing does not improve the results of classification. Using MobileNetV2, the significance of pre-processing can be noticed properly. In this case, the pre-processing of the image increases the accuracy, sensitivity, specificity, precision, and F1-score. Adding the wavelet features increases the results significantly. Using DenseNet121 and Wavelet features (with pre-processing) the accuracy is about 96.15% whereas the accuracy is increased to 97.73% using MobileNetV2 and wavelet features (with pre-processing). Though MobileNetV2 is smaller in size, the dimension of the feature set is increased. For this reason, the accuracy is much better-using MobileNetV2 for the increased dimension.

As the model is proposed for the main utilization of telemedicine platforms and Mobile health care, memory consumption is examined to ensure the ability of the model to run online or in devices with lower memory support. From Table I, we observe that memory requirement increases with the addition of wavelet transformation. Table II gives a comparison in terms of the number of trainable parameters,

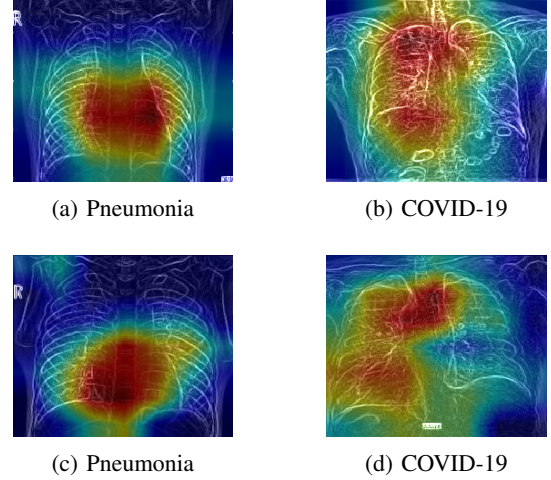


Fig. 2: Class-activation heatmaps are generated, where (a), (b) are using DenseNet121 and (c), (d) are using MobileNetV2.

non trainable parameters, extracted features, memory size, and time required for the classification. As the number of extracted features of the model which uses MobileNetV2 for feature extraction is higher, it requires more time to train the model. Thus, the combination of pre-processing, wavelet, and MobileNetV2 provide better results and lower memory requirement in comparison to other combination. It can be concluded that the combination of pre-processing with MobileNetV2 and wavelet is better than the one using DenseNet121 in conjunction with pre-processing and wavelet transform. Our proposed method is better than existing methods as it provides higher accuracy, lower memory requirement, and feature details of the x-ray images. There is a scope of improvement by increasing the number of chest x-ray images.

IV. CONCLUSION

In this work, we have proposed a method of chest x-ray image classification using wavelet transform and DenseNet121/MobileNetV2 based features in order to identify COVID-19 pneumonia. The images have been pre-processed using histogram equalization and edge-detection. Subsequently, features are extracted from wavelet decomposition and two different pre-trained neural networks, namely MobileNetV2 and DenseNet121. The features have been extracted from publicly available 2,940 chest x-ray images

TABLE II: Parameters and Time analysis of 3 class classification for two different setups

Method	Total Parameters	Trainable Parameters	Non-trainable Parameters	Extracted Features	Time	Size
Preprocessing+Wavelet+DenseNet121	7,037,504	6,953,856	83,648	100,352	5min 8sec	2520.79 MB
Preprocessing+Wavelet+MobileNetV2	2,257,984	2,223,872	34,112	112,896	5min 17sec	2468.66 MB

containing 940 cases of COVID-19 pneumonia. It has been shown that using pre-processing and wavelet-based features in conjunction with the neural network-based features can yield superior detection as compared to using the latter only. Overall, the best performance has been obtained employing MobileNetV2 with pre-processing and wavelet transform followed by the use of DenseNet121 because of the higher feature dimension of the former. The computational performance of the different approaches has also been analyzed. There is scope for further investigations using additional COVID-19 positive chest x-ray images and wavelet transforms with improved directionalities and redundancy.

REFERENCES

- [1] T. A. Ghebreyesus, "Who Director-General's opening remarks at the media briefing on COVID-19-11 march 2020," *World Health Organization*, 2020.
- [2] S. P. Adhikari, S. Meng, Y.-J. Wu, Y.-P. Mao, R.-X. Ye, Q.-Z. Wang, C. Sun, S. Sylvia, S. Rozelle, H. Raat *et al.*, "Epidemiology, causes, clinical manifestation and diagnosis, prevention and control of coronavirus disease (COVID-19) during the early outbreak period: a scoping review," *Infectious diseases of poverty*, vol. 9, no. 1, pp. 1–12, 2020.
- [3] K. Dutta, S. Shityakov, O. Morozova, I. Khalifa, J. Zhang, A. Panda, and C. Ghosh, "Beclabuvir can inhibit the RNA-dependent RNA polymerase of newly emerged novel coronavirus (SARS-CoV-2)," 2020.
- [4] C. Avery, W. Bossert, A. Clark, G. Ellison, and S. F. Ellison, "Policy Implications of Models of the Spread of Coronavirus: Perspectives and Opportunities for Economists," National Bureau of Economic Research, Tech. Rep., 2020.
- [5] W. Wang, Y. Xu, R. Gao, R. Lu, K. Han, G. Wu, and W. Tan, "Detection of SARS-CoV-2 in different types of clinical specimens," *Jama*, 2020.
- [6] C. Huang, Y. Wang, X. Li, L. Ren, J. Zhao, Y. Hu, L. Zhang, G. Fan, J. Xu, X. Gu *et al.*, "Clinical features of patients infected with 2019 novel coronavirus in wuhan, china," *The lancet*, vol. 395, no. 10223, pp. 497–506, 2020.
- [7] V. M. Corman, O. Landt, M. Kaiser, R. Molenkamp, A. Meijer, D. K. Chu, T. Bleicker, S. Brünink, J. Schneider, M. L. Schmidt *et al.*, "Detection of 2019 novel coronavirus (2019-nCoV) by real-time RT-PCR," *Eurosurveillance*, vol. 25, no. 3, p. 2000045, 2020.
- [8] D. K. Chu, Y. Pan, S. M. Cheng, K. P. Hui, P. Krishnan, Y. Liu, D. Y. Ng, C. K. Wan, P. Yang, Q. Wang *et al.*, "Molecular diagnosis of a novel coronavirus (2019-nCoV) causing an outbreak of pneumonia," *Clinical chemistry*, vol. 66, no. 4, pp. 549–555, 2020.
- [9] M. Chung, A. Bernheim, X. Mei, N. Zhang, M. Huang, X. Zeng, J. Cui, W. Xu, Y. Yang, Z. A. Fayad *et al.*, "CT imaging features of 2019 novel coronavirus (2019-nCoV)," *Radiology*, vol. 295, no. 1, pp. 202–207, 2020.
- [10] S. Salehi, A. Abedi, S. Balakrishnan, and A. Gholamrezaezhad, "Coronavirus disease 2019 (COVID-19): a systematic review of imaging findings in 919 patients," *American Journal of Roentgenology*, pp. 1–7, 2020.
- [11] H. Y. F. Wong *et al.*, "Frequency and distribution of chest radiographic findings in COVID-19 positive patients," *Radiology*, p. 201160, 2020.
- [12] I. D. Apostolopoulos and T. A. Mpesiana, "Covid-19: automatic detection from x-ray images utilizing transfer learning with convolutional neural networks," *Physical and Engineering Sciences in Medicine*, p. 1, 2020.
- [13] A. Narin, C. Kaya, and Z. Pamuk, "Automatic detection of coronavirus disease (covid-19) using x-ray images and deep convolutional neural networks," *arXiv preprint arXiv:2003.10849*, 2020.
- [14] L. Wang and A. Wong, "Covid-net: A tailored deep convolutional neural network design for detection of covid-19 cases from chest radiography images," *arXiv preprint arXiv:2003.09871*, 2020.
- [15] P. Afshar, S. Heidarian, F. Naderkhani, A. Oikonomou, K. N. Plataniotis, and A. Mohammadi, "Covid-caps: A capsule network-based framework for identification of covid-19 cases from x-ray images," *arXiv preprint arXiv:2004.02696*, 2020.
- [16] T. Mahmud, M. A. Rahman, and S. A. Fattah, "CovXNet: A multi-dilation convolutional neural network for automatic COVID-19 and other pneumonia detection from chest X-ray images with transferable multi-receptive feature optimization," *Computers in biology and medicine*, vol. 122, p. 103869, 2020.
- [17] X. Li, C. Li, and D. Zhu, "COVID-MobileXpert: On-Device COVID-19 Screening using Snapshots of Chest X-Ray," *arXiv preprint arXiv:2004.03042*, 2020.
- [18] *COVID-19 Radiography Database — Kaggle*, 2020 (accessed October 2, 2020). [Online]. Available: <https://www.kaggle.com/tawsifurrahman/covid19-radiography-database>
- [19] J. P. Cohen, P. Morrison, L. Dao, K. Roth, T. Q. Duong, and M. Ghassemi, "COVID-19 Image Data Collection: Prospective Predictions are the Future," 2020.
- [20] *Devakumar kp — Kaggle*, 2020 (accessed August 5, 2020). [Online]. Available: <https://www.kaggle.com/imdevskp>
- [21] R. B. Jeyavathana, R. Balasubramanian, and A. A. Pandian, "A survey: analysis on preprocessing and segmentation techniques for medical images," *International Journal of Research and Scientific Innovation (IJRSI)*, 2016.
- [22] H. Behzadi-khormouji, H. Rostami, S. Salehi, T. Derakhshande-Rishehri, M. Masoumi, S. Salemi, A. Keshavarz, A. Gholamrezaezhad, M. Asadi, and A. Batouli, "Deep learning, reusable and problem-based architectures for detection of consolidation on chest x-ray images," *Computer methods and programs in biomedicine*, vol. 185, p. 105162, 2020.
- [23] K. Zuiderveld, "Contrast limited adaptive histogram equalization," in *Graphics gems IV*. Academic Press Professional, Inc., 1994, pp. 474–485.
- [24] O. Miljković, "Image pre-processing tool," *Kragujevac Journal of Mathematics*, vol. 32, no. 32, pp. 97–107, 2009.
- [25] O. R. Vincent, O. Folorunso *et al.*, "A descriptive algorithm for sobel image edge detection," in *Proceedings of Informing Science & IT Education Conference (InSITE)*, vol. 40. Informing Science Institute California, 2009, pp. 97–107.
- [26] G. Huang, Z. Liu, L. van der Maaten, and K. Weinberger, "Densely Connected Convolutional Networks," 07 2017.
- [27] M. Sandler, A. Howard, M. Zhu, A. Zhmoginov, and L.-C. Chen, "MobileNetV2: Inverted residuals and linear bottlenecks," in *CVPR*, 2018, pp. 4510–4520.
- [28] Q. Xiang, X. Wang, R. Li, G. Zhang, J. Lai, and Q. Hu, "Fruit Image Classification Based on MobileNetV2 with Transfer Learning Technique," in *Proceedings of the 3rd International Conference on Computer Science and Application Engineering*, 2019, pp. 1–7.
- [29] T. Ozturk, M. Talo, E. A. Yildirim, U. B. Baloglu, O. Yildirim, and U. R. Acharya, "Automated detection of COVID-19 cases using deep neural networks with x-ray images," *Computers in Biology and Medicine*, p. 103792, 2020.
- [30] *TheRadiologyAssistant:COVID19-Imaging-Findings*, 2020 (accessed October 2, 2020). [Online]. Available: <https://radiologyassistant.nl/chest/covid-19/covid19-imaging-findings>